Ecological Indicators 150 (2023) 110211

Contents lists available at ScienceDirect

Ecological Indicators

journal homepage: www.elsevier.com/locate/ecolind

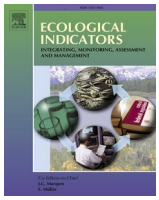

Original Articles

Spatiotemporal changes in landscape patterns in karst mountainous regions based on the optimal landscape scale: A case study of Guiyang City in Guizhou Province, China

Changyue Hu [a], Wu Wu [a], Xuexia Zhou [a], Zhijie Wang [a,b,*]

[a] Key laboratory of Plant Resource Conservation and Germplasm Innovation in Mountainous Region (Ministry of Education), College of Life Sciences/Institute of Agro-bioengineering, Guizhou University, Guiyang 550025, Guizhou Province, China
[b] Collaborative Innovation Center for Mountain Ecology & Agro-Bioengineering, Guizhou University, Guiyang 550025, Guizhou Province, China

ARTICLE INFO

Keywords:
Landscape pattern
Landscape index
Scale effect
Karst mountainous city
Guiyang City

ABSTRACT

The accurate analysis of landscape pattern and ecological process characteristics in rapidly urbanized areas is crucial for formulating policies related to differentiated urban development and landscape management measures. However, there are no convincing set of overall indices suitable and the optimal scale in karst mountainous regions. This study determined optimal landscape indices and scales and analysed the temporal and spatial variation characteristics of landscape patterns in the karst mountainous city of central Guizhou Province by taking Guiyang City as a case study area using Principal component analysis and inflection point analysis. The results show that: (1) the nine landscape indices (i.e., edge density (ED), mean radius of gyration (GYRATE_MN), mean contiguity index (CONTIG_MN), mean shape index (SHAPE_MN), contagion index (CONTAG), interspersion and juxtaposition index (IJI), Shannon's diversity index (SHDI), proportion of urban area (UI), Gibbs-Martin diversity index(GM)) were optimal indices of landscape pattern analysis in karst mountainous cities, with optimal landscape grain and extent of 90 m and 1000 m, respectively; (2) from 1995 to 2019, the landscape pattern in karst mountainous region has changed dramatically under the impact of rapid urbanization, and urbanization and ecologization were main trends of landscape pattern changes; and (3) the landscape fragmentation was intensified with the regularity tendency of patch shape, which is still facing severe challenges to the protection of regional ecological environment. This study makes important contributions to exploring the response between landscape pattern changes and ecological processes and promoting ecological sustainable development in karst mountain cities.

1. Introduction

Landscape patterns are defined as spatial arrangements of various landscape elements of different sizes and shapes (Dadashpoor and Salarian, 2020). Changes in landscape patterns are mainly observed through changes in land use/land cover (Křováková et al., 2015). It could connect land cover to human activities that alter landscape patterns and structures. Among them, human activities such as urban expansion, afforestation, and deforestation play a vital role in the characteristics of landscape patterns (Abbas et al., 2022; Song et al., 2022). In addition, the characteristics of landscape patterns, known as landscape or spatial heterogeneity can influence ecological processes with profound impacts on the functioning of ecological and socioeconomic systems (Cushman et al., 2010; Lausch et al., 2015). Over the past few decades, many previous studies have considered the landscape pattern changes and their driving forces, especially in plain regions and urban areas. For example, Zheng et al. (2022) used the landscape indices to conduct a detailed study on the driving mechanism of spatiotemporal patterns in the Huang-Huai-Hai Plain. Yuan et al. (2021) studied the spatiotemporal characteristics in landscape patterns in the core area of urbanization, which is between Zhengzhou City and Kaifeng City in China. In recent years, some scholars have studied the characteristics in landscape patterns in Southwest China. For example, Liu et al. (2022c) explored the spatiotemporal evolution in landscape patterns in the Guangxi Zhuang Autonomous Region and analysed the relationship between landscape patterns and ecosystem service

* Corresponding author at: College of Life Sciences, Guizhou University, Huaxi District, Guiyang City, Guizhou Province 550025, China.
E-mail address: zjwang3@gzu.edu.cn (Z. Wang).

https://doi.org/10.1016/j.ecolind.2023.110211
Received 6 May 2022; Received in revised form 17 February 2023; Accepted 1 April 2023
Available online 5 April 2023

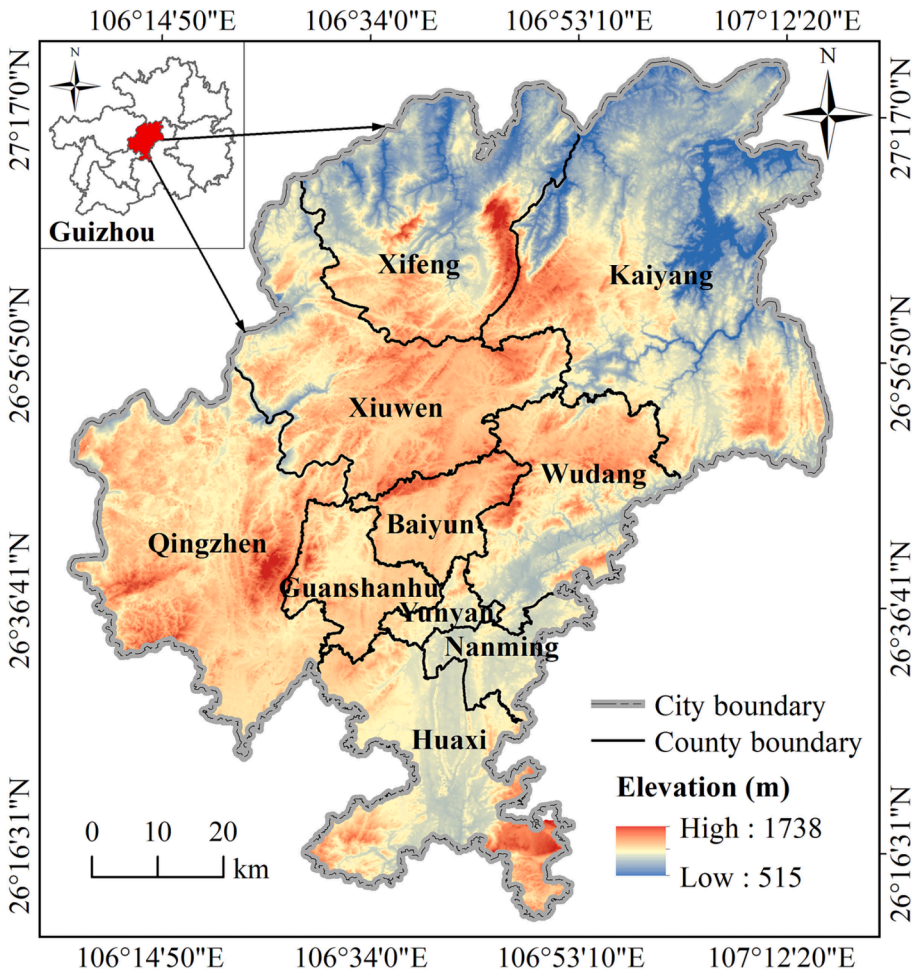

Fig. 1. Location of Guiyang City.

function. However, the relatively little research has been conducted in the rapidly urbanized southwestern regions, especially in the karst mountainous cities.

Landscape indices can be used to quantitatively reflect the complex structure, spatial configuration and other characteristics (Cheung et al., 2016; Li et al., 2020). The core goal in studying changes in landscape patterns is to strengthen the combination of landscape indices and ecological processes to improve the scientific nature of pattern analysis (Li and Wu, 2004; Zhang et al., 2020). Several studies had used landscape indices to analyse landscape patterns. For example, Mohamed et al. (2021) found that a total of eight indices were the optimal metric to evaluated the spatial patterns of landscape structure. The landscape scale reflects the spatial heterogeneity of a landscape and it is used as a research core of landscape ecology (Fu et al., 2011). Since the landscape indices are highly dependent on the observation scale, the scale effect of landscape patterns must be considered in studies (Fang et al., 2017). The relationship between landscape indices and scale has been considered in the previous studies, but the optimal landscape scale obtained varies. For example, Yuan et al. (2021) found that the optimal grain was 120 m in Hangzhou city with rapid urbanization. Wang et al. (2021b) found that the optimal grain was 60 m to analysis landscape patterns in Shanghai City. Moreover, due to the high correlation and redundancy between landscape indices and the difference of research objects and purposes, the optimal landscape indices are often distinct (Jia et al., 2019; Wang et al., 2021b). In addition, the optimal scales for analyzing landscape pattern characteristics are different due to data source differences and heterogeneity of landscapes in different regions (Wang et al., 2018). Currently, researchers typically refer directly to previous studies for selecting indices, which is easy to leads to a certain degree of blind obedience, and the persuasion in describing the landscape pattern is not strong (Kupfer, 2012). Therefore, it is of great significance to select the optimal landscape indices and scale for effectively promoting sustainable landscape planning and management (Tian et al., 2019).

Along with the rise of extensive landscape changes and urbanization around the world, especially in developing countries, this phenomenon has increased in karst mountainous areas in recent decades and has led to widespread changes in the spatial pattern of the landscape (Liu et al., 2022b). Guiyang City is located in the centre of the Yunnan-Guizhou Plateau in southern China, which is the most typical and complex karst region in the world (Chen et al., 2021a). In addition, carbonates form soil slowly due to the high solubility and low acid-insoluble matter content of widely distributed carbonate rocks (Gong et al., 2021). Meanwhile, the region is characterized by broken surfaces, poor regulation and water conservation, and complex and diverse microlandforms that are affected and constrained by the special geological contexts and climatic conditions (Hu et al., 2020; Xiao et al., 2023; Zhang et al., 2020; Zhang et al., 2022). Consequently, there are many ecological problems, such as high rock exposure rate, thin karst soil layer, serious soil erosion and water resource shortage, and it has become the largest and most concentrated ecologically fragile area (Liu et al., 2022a; Xiao et al., 2023; Zhang et al., 2022; Zhang et al., 2021). In the process of urbanization in the mountainous areas, the significant decrease of vegetation coverage was caused by the encroachment of construction land on cultivated land and woodland (Liu et al., 2022a). As urbanization in mountainous regions concentrates in intermountain hills formed by various geomorphological processes, single and

continuous natural patches have become complex, heterogeneous and discontinuous mosaics (Li et al., 2017). In addition, ecological projects have huge impacts on vegetation restoration, which caused the large-scale transformation of land use types (Liu et al., 2022a). Several ecological restoration projects and studies on ecological protection have been carried out to quantify the impacts of ecological projects on the local ecological environment and improve the fragile ecological environment (Gong et al., 2021). These changes had some impact on landscape patterns and ecological environments. Therefore, quantifying landscape patterns and their changes is essential for the monitoring and assessment of the ecological consequences of urbanization and subsequent decision-making.

There are significant differences in the ability of different landscape indices to measure characteristics of landscape patterns. However, to the best of our knowledge, there are no set of overall indices suitable and the optimal scale for karst urban landscapes and applied to landscape pattern analysis in the study of urban landscape patterns, especially in karst areas with fragile ecological environments. Therefore, in this study, Guiyang City was selected as the research area to determine a set of landscape indices suitable for karst cities and analyse the spatiotemporal characteristics of landscape patterns in the study area to provide theoretical support for ecologically sustainable regional planning. The aims of this study were (1) to reveal reasonable landscape indices for landscape pattern analysis in karst mountainous regions; (2) to determine the optimal landscape scale (grain and extent) of karst landscape pattern analysis; and (3) to reveal the landscape pattern changes in Guiyang City from 1995 to 2019 based on the optimal landscape indices and scale.

2. Materials and methods

2.1. Study area

Guiyang City (106°07′–107°17′E, 26°11′–26°55′N), located in the middle of the Yunnan-Guizhou Plateau and Guizhou Province (Fig. 1), and contains one county-level city, three counties, and six districts, with an area of 8043.37 km^2 (Luo et al., 2022; Wang et al., 2022). The climate type in the region is a subtropical monsoon climate with an average annual temperature and precipitation of 15.3 ℃ and 1197–1248 mm, respectively (Wang et al., 2022). The geomorphology of the area consists of a hilly karst basin area dominated by mountains and hills, with an elevation of 1180 m. The terrain of the area is generally high in the southwest and low in the northeast (Chen et al., 2021b). The karst basin, valley and eroded depression are covered with clustered hills, and the karst environment is fragile (Zhou et al., 2022). Under the guidance of the overall urban planning of Guiyang City (1996–2010) and (2011–2020) approved by the Stats Council since 1990, Guiyang City has entered the stage of rapid development and the urbanization rate increased from 58.12% in 1995 to 78.80% in 2019 (Wang et al., 2022; Yang et al., 2020). Although the province's economy is relatively underdeveloped, Guiyang's GDP has grown exponentially, and the total population of 5.99 million in 2019 according to official statistics (Bai et al., 2023; Liao et al., 2022). Under the guidance of the plan for constructing a national demonstration city of ecological civilization in Guiyang (2012–2020) approved by the States Council in 2012, Guiyang City has continuously strengthened its efforts to protect the ecological environment and aims for sustainable ecological development (Peng et al., 2015). Under the coupling effect of economic development and environmental protection, intense human activities and special geological conditions have induced drastic changes in landscape patterns, which affected the stability and natural recovery ability of karst ecology, and brought challenges to local economic development and environmental protection (Chen et al., 2022; Dai and Wang, 2023). The city is chosen as the study area, because it is a typical karst vulnerable area and an important central city in Southwest China (Li et al., 2022b; Liu et al., 2022b). Additionally, this area is also the capital city of Guizhou Province, which has rich forestry resources and a high forest carbon sink capacity, contributing to the global carbon sink (Bai et al., 2023). Studying the spatiotemporal characteristics in landscape patterns can provide a reference for the ecological restoration of karst areas, which is of great significance for promoting coordinated regional low-carbon development, and achieving the sustainable goal of "economy and ecology".

Table 1
Landsat image data used in the study.

Year	Satellite	Sensor	Date	Path/Row
1995	Landsat-5	TM	Sep. 1995	127/41, 127/42
2000	Landsat-5	TM	Dec. 1999	127/41, 127/42
2005	Landsat-5	TM	Dec. 2004	127/41, 127/42
2010	Landsat-5	TM	Sep. 2009	127/41, 127/42
2015	Landsat-8	OLI-TIRS	Dec. 2015	127/41, 127/42
2019	Landsat-8	OLI-TIRS	Sep. 2019	127/41, 127/42

2.2. Data collection and processing

2.2.1. Data source

In this study, the main sources of data were Landsat-5 Thematic Mapper (TM) images for 1995, 2000, 2005 and 2010 and Landsat-8 Operational Land Imager (OLI) images for 2015 and 2019. Remote satellite images and digital elevation model (DEM) were collected from the website of the United States Geological Survey (USGS) (https://glouvis.usgs.gov/) and geographical spatial data (https://www.gscloud.cn/). The road density data are derived from the OpenStreetMap platform (https://www.openstreetmap.org/). The cloud content of all of the remote images was less than 5% with a spatial resolution of 30 m × 30 m, and the image quality was good. In addition, the coordinate system of all images was uniformly resampled to the WGS_1984_UTM_Zone_48N projection coordinate system. The information on satellite orbital parameters is listed in Table 1.

2.2.2. Data processing

First, the fast line-of-sight atmospheric analysis of spectral hypercubes (FLAASH) module in environment for visualizing images (ENVI) 5.3 software was applied for radiometric and atmospheric correction (Wang et al., 2019). Radiometric calibration parameters exist in metadata files and can be read automatically using Radiometric Correction tools in ENVI software. Second, considering the different sources of Landsat images, the best band combination was selected according to the principle of high separability. Then, geometric corrections were performed on the satellite images in ENVI 5.3 software based on a 1:10,000 topographical map obtained from the Bureau of Surveying, Mapping and Geographic Information of Guizhou Province. For the classification, the Landsat-8 OLI images in 2015 and 2019 were selected short wave infrared (SWIR), near-infrared (NIR) and green bands, and the Landsat-5 TM images in 1995, 2000, 2005 and 2010 were selected SWIR, NIR and red bands. Furthermore, according to China's land use classification standard (GB/T 21010–2017) and interpreted by the combination of the support vector machine supervised classification method and manual visual interpretation, the land use types were classified into 6 categories, including cultivated land, woodland, grassland, construction land, waterbody and unused land. Support vector machine is able to classify the data based on a very sophisticated statistical spatial analysis, identifying each land use type to its highest accuracy (Ul Din and Mak, 2021). For each land-use type, a sufficient number of training samples were first collected through visual interpretation of remote sensing images. Then, the separability test of the selected samples was implemented to ensure the independence of the samples. Finally, the confusion matrix method based on random points was used to ensure the accuracy of data classification. Two hundred points in each image were selected from high-resolution images of

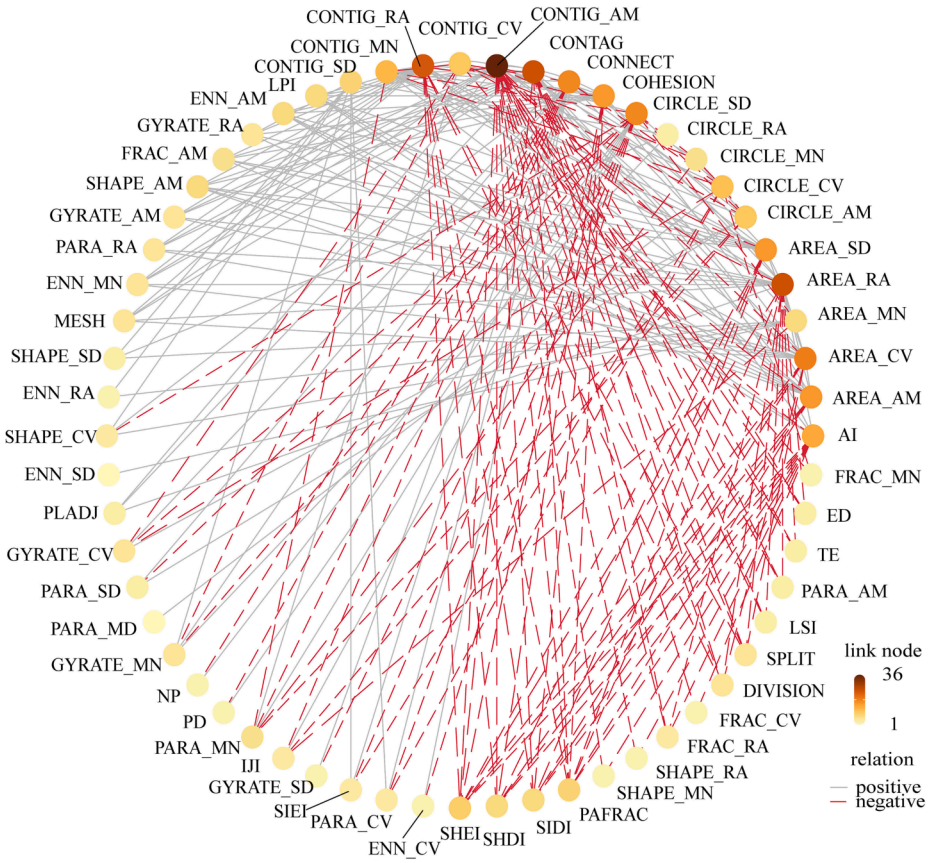

Fig. 2. Correlation network diagram of landscape indices ***Notes:*** Aggregation Index (AI); Patch area (AREA); Related circumscribing circle (CIRCLE); Patch cohesion index (COHESION); Connectance index (CONNECT); Contagion index (CONTAG); Contiguity index (CONTIG); Landscape division index (DIVISION); Edge density (ED); Euclidean nearest neighbour distance (ENN); Fractal dimension index (FRAC); Radius of gyration (GYRATE); Interspersion and Juxtaposition index (IJI); Largest patch index (LPI); Landscape shape index (LSI); Effective mesh size (MESH); Number of patches (NP); Perimeter area fractal dimension index (PAFRAC); Perimeter-area ratio (PARA); Patch density (PD); Percentage of like adjacencies (PLADJ); Shape index (SHAPE); Shannon's diversity index (SHDI); Shannon's evenness index (SHEI); Simpson's diversity index (SIDI); Simpson's evenness index (SIEI); Splitting index (SPLIT); Total Edge (TE). AM, CV, MD, MN, RS, and SD are area-weighted mean, coefficient of variation, median, mean, range, and standard deviation for every landscape index, respectively.

Google history images to verify the accuracy, and the Kappa index was calculated to evaluate the accuracy of classification images (Xu et al., 2019). The overall classification accuracy of each period and the classification accuracy of each land use type were more than 85%, with a Kappa coefficient greater than 0.75.

2.3. Methods

2.3.1. Calculation of landscape indices

Landscape indices are one of the most effective methods to quantify landscape pattern characteristics. Due to the complexity and diversity of landscape indices, reasonable selection of the landscape pattern index is the key to scientific landscape pattern analysis. FRAGSTATS is a widely used landscape pattern analysis software that has powerful calculation and analysis functions. It can calculate three levels of landscape indices, namely, patch, class, and landscape (Alhamad et al., 2011). This study focused on the characteristics of different landscape types and the overall landscape in the study area. Accordingly, sixty-nine of the most representative used landscape level indices were calculated using FRAGSTATS 4.2. In addition, ArcGIS was used to process and calculate the Gibbs Martin diversity index, topographic position index, proportion of woodland, which can represent characteristics in karst mountainous regions, and proportion of urban area and road density, which can represent urbanization (Li et al., 2022b; Maity et al., 2021). These indices generally represented six main aspects of landscape structure, namely, "area/perimeter/density", "diversity", "shape", "contagion", "karst traits" and "urbanization".

2.3.2. Correlation analysis and principal component analysis

Due to the strong correlation between some indices, information redundancy may occur in landscape pattern analysis. The principal component analysis can reduce multidimensional data to lower dimensions, while retaining most of the information, by using orthogonal transformation to convert a set of observations of possibly correlated variables into a set of values of linearly uncorrelated variables (Migenda et al., 2021). The larger the contribution rate of the principal component, the more content the initial variable represented (Yang and Wang, 2021). Therefore, the landscape indices with high correlation were eliminated through correlation analysis to reduce the information redundancy. Then, we employed principal component analysis to determine the optimal indices of among landscape indices by identifying the core landscape indices which explained the landscape variability.

2.3.3. Scaling-up and inflection point analysis

For grain size analysis, selecting the landscape type dataset in 2019 as the sample, the resampling method in ArcGIS 10.5 was used to resample the grid size ranging from the original spatial resolution of 30 m to the maximum of 300 m with 10 m increments. Under the optimal particle size, the moving window method was used to analyse the extent effect of the landscape indices, and can further observe the fragmentation and spatial variation of landscape pattern. As landscape pattern analysis is dependent on scale, a smaller scale always ignores the complexity of landscape function and structure, and a larger scale simplifies input parameters. According to the landscape index changes greatly near the inflection point, in this study, the inflection point analysis method was used to comprehensively analyse the change trend of landscape indices with grain and extent and determine the first scale domain according to the obvious scale turning point (Fu et al., 2021).

2.3.4. Information loss evaluation model

To measure the overall information loss degree of landscapes in the resampling process and further determine the optimal scale, the grid size in the first scale domain was used as the abscissa. Meanwhile, the change value of the regional land area was used as the ordinate for graphical

Table 2
List of landscape indices used in the study.

Landscape indices	Abbreviation	Landscape indices	Abbreviation
Patch density	PD	Area-weighted mean shape index	SHAPE_AM
Largest patch index	LPI	Standard deviation in shape index	SHAPE_SD
Edge density	ED	Mean fractal dimension index	FRAC_MN
Coefficient of variation in patch area	AREA_CV	Area-weighted mean fractal dimension index	FRAC_AM
Mean radius of gyration	GYRATE_MN	Mean contiguity index	CONTIG_MN
Coefficient of variation in radius of gyration	GYRATE_CV	Standard deviation index in contiguity index	CONTIG_SD
Shannon's diversity index	SHDI	Landscape shape index	LSI
Contagion index	CONTAG	Area-weighted mean related circumscribing circle	CIRCLE_AM
Interspersion and Juxtaposition index	IJI	Connectance index	CONNECT
Perimeter area fractal dimension index	PAFRAC	Proportion of urban area	UI
Mean shape index	SHAPE_MN	Gibbs-Martin diversity index	GM

Table 3
Eigenvalues and proportion of total variance and cumulative variance based on principal components analysis.

Groups	Factor	Eigenvalues	Variance (%)	Cumulative variance (%)
Area/Perimeter/ Density	1	4.027	67.123	67.123
	2	1.789	29.818	96.941
Shape	1	5.607	62.297	62.297
	2	2.948	32.754	95.051
Contagion	1	2.984	74.607	74.607
	2	0.860	21.510	96.117

analysis. The information loss evaluation model was adopted here (Xu et al., 2012):

$$L_i = (A_i - A_{bi})/A_{bi} \times 100 \quad (1)$$

$$S = \sqrt{\frac{\sum_{i=1}^{n} L_i^2}{n}} \quad (2)$$

where L_i refers to the relative value of area loss, n is the total number of landscape types, S refers to the total value of area loss, and A_i and A_{bi} refer to the area of a type after scale conversion and before scale conversion, respectively.

3. Results

3.1. Optimal landscape indices and scale in karst mountainous regions

3.1.1. Optimal landscape indices

The results showed that there was a strong correlation among landscape indices in the correlation analysis (Fig. 2). Fifty-two out of the original seventy-four highly correlated indices were eliminated, leaving only twenty-two representative indices (Table 2). The results of principal component analysis showed that the cumulative contribution of the first two components of the area/perimeter/density index, shape index and contagion index reached 96.941%, 95.051% and 96.117%, which could essentially reflect most of the information of the original

Table 4
Principal component eigenvector and load.

Group	Landscape indices	Eigenvector		Load	
		1	2	1	2
Area/Perimeter/ Density	PD	−0.976	0.209	−1.959	0.280
	LPI	0.736	0.631	1.477	0.844
	ED	−0.977	−0.057	−1.961	−0.076
	AREA_CV	0.647	0.747	1.298	0.999
	GYRATE_MN	0.560	−0.800	1.124	−1.070
	GYRATE_CV	0.920	0.382	1.846	−0.511
Shape	SHAPE_MN	0.370	0.922	0.876	1.583
	SHAPE_AM	0.696	−0.635	1.648	−1.090
	SHAPE_SD	0.684	0.661	1.620	1.135
	FRAC_MN	0.545	0.822	1.291	1.411
	FRAC_AM	0.877	−0.472	2.077	−0.810
	CONTIG_MN	0.994	−0.048	2.354	−0.082
	CONTIG_SD	0.992	−0.097	2.349	−0.167
	LSI	−0.816	0.571	−1.932	0.980
	CIRCLE_AM	0.904	0.145	2.141	0.249
Contagion	CONTAG	0.895	0.427	1.546	0.396
	IJI	−0.803	0.546	−1.387	0.506
	CONNECT	0.873	−0.404	1.508	−0.375
	PAFRAC	−0.881	−0.465	−1.522	−0.431

Notes: Patch density (PD); Largest patch index (LPI); Edge density (ED); Coefficient of variation in patch area (AREA_CV); Mean radius of gyration (GYRATE_MN); Coefficient of variation in radius of gyration (GYRATE_CV); Mean shape index (SHAPE_MN); Area-weighted mean shape index (SHAPE_AM); Standard deviation in shape index (SHAPE_SD); Mean fractal dimension index (FRAC_MN); Area-weighted mean fractal dimension index (FRAC_AM); Mean contiguity index (CONTIG_MN); Standard deviation index in contiguity index (CONTIG_SD); Landscape shape index (LSI); Area-weighted mean related circumscribing circle (CIRCLE_AM); Contagion index (CONTAG); Interspersion and Juxtaposition index (IJI); Connectance index (CONNECT); Perimeter area fractal dimension index (PAFRAC).

indices (Table 3). Among them, in the area/perimeter/density indices, the first and second principal components generated the highest loadings for edge density (ED) (-1.961) and mean radius of gyration (GYRATE_MN) (-1.070), respectively. In the shape indices, the first and second principal components generated the highest loadings for mean contiguity index (CONTIG_MN) (2.354) and mean shape index (SHAPE_MN) (-1.583), respectively. In the area of contagion indices, the first and second principal components generated the highest loadings for contagion (CONTAG) (1.546) and Interspersion and Juxtaposition index (IJI) (0.506), respectively (Table 4). We selected the index that produced the highest loading of principal components. In addition, Shannon's diversity index (SHDI), proportion of urban area (UI) and Gibbs-Martin diversity index (GM) were selected from landscape diversity, urbanization and indices of karst traits, respectively. Therefore, nine indices were selected for subsequent analysis.

3.1.2. Optimal landscape grain

There are four types of response curves for the 9 indices (Fig. 3). Type 1 was the relation of concave curve. These response curves correspond to SHAPE_MN, CONTAG and COTIG_MN (Fig. 3(a and b)). The change trend of the indices showed an overall downtrend with the rapidly changing speed at 30–90 m. As the grain size increased, these curves were flattened after 120 m. Type 2 was the relation of no-law scaling. With changing grain size, the IJI response curves showed small-amplitude fluctuations, while the UI and GM response curves remained basically unchanged without obvious regularity (Fig. 3(b and c)). Type 3 was the relation of sensitivity. A significant scale effect was not observed for SHDI in the diversity indices at 30–120 m, whereas SHDI had great change with irregular fluctuation after 120 m (Fig. 3(c)). Type 4 was the relation of monotone function. These response curves correspond to ED and GYRATE_MN, showing a monotonic increasing or decreasing trend with an inconspicuous inflection point (Fig. 3(d)). Since most of indices were sensitive to the grain size of 30 to 120 m,

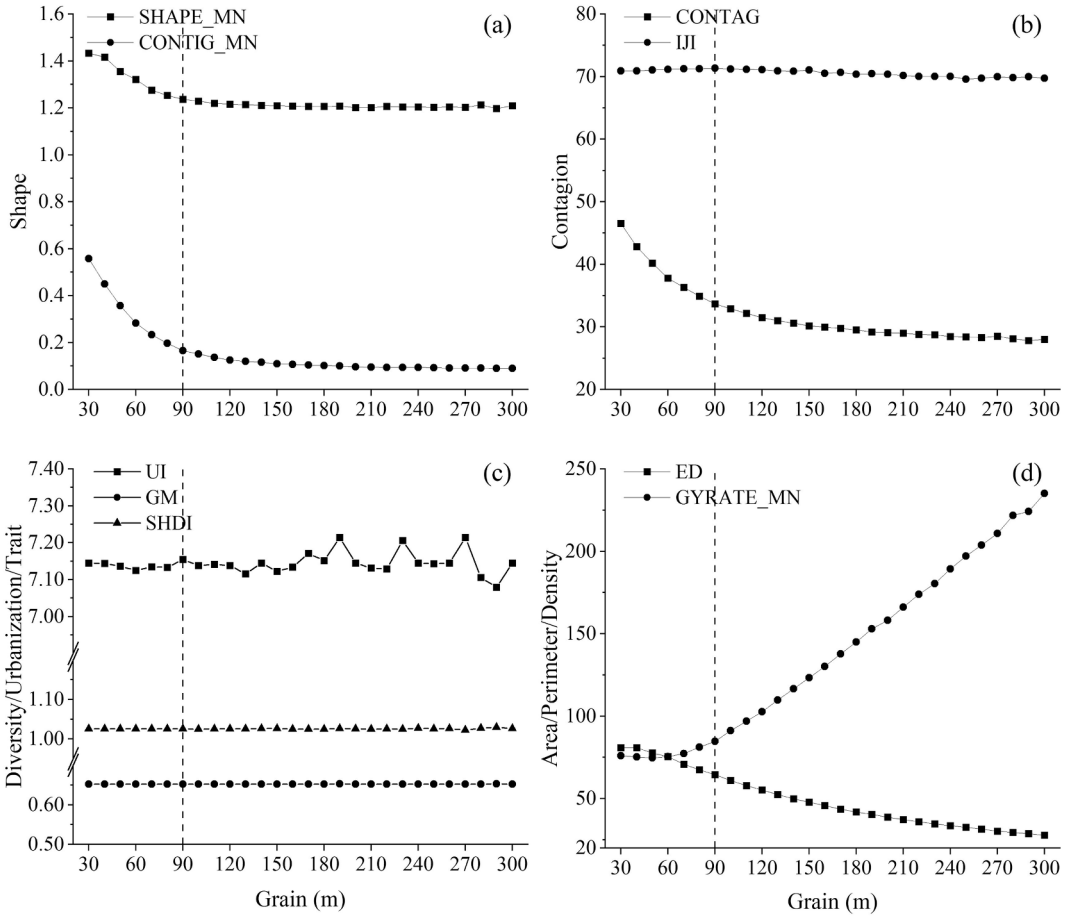

Fig. 3. Landscape indices for various grain sizes ***Notes:*** Edge density (ED); Mean radius of gyration (GYRATE_MN); Contagion index (CONTAG); Interspersion and Juxtaposition index (IJI); Mean contiguity index (CONTIG_MN); Mean shape index (SHAPE_MN); Shannon's diversity index (SHDI); Proportion of urban area (UI); Gibbs-Martin diversity index (GM).

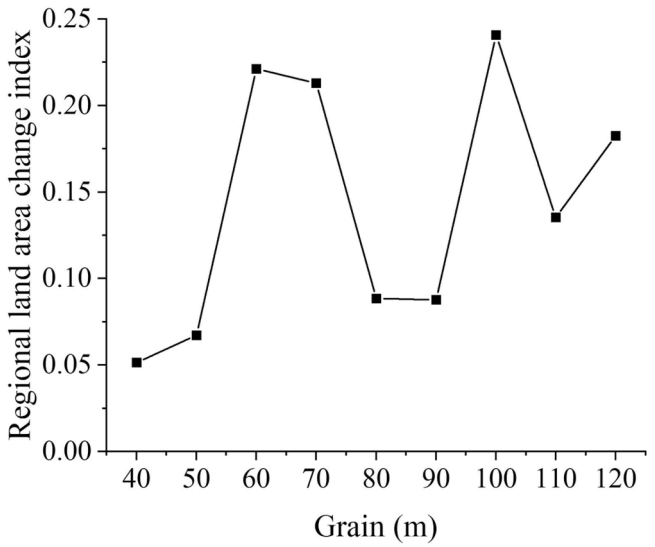

Fig. 4. Information loss of landscape types for different grain sizes.

30–120 m was identified as the first scale domain.

Following the method described in Formulas (1) and (2), we calculated the information loss for the first scale domain. Overall, information loss fluctuates with increasing grain size (Fig. 4). When the grid resolution was between [30, 50] and [80, 90], the information loss was smaller than other resolutions, which was less than 0.10 in both. Slightly larger grains should be selected as an optimal scale in the first scale domain, which reflects better landscape characteristic information while requiring less data-processing time (Wang et al., 2021b). The optimal grain of landscape patterns analysis in this study was 90 m based on the results of grain effect analysis and information loss evaluation.

3.1.3. *Optimal landscape extent*

Under the optimal particle size of 90 m, the moving window method was used to analyse the extent effect of the landscape indices. We used the interval of 180 m as the size of the moving window and set 17 grades from 270 m to 3150 m. With increasing extent, there were two types of response curves (Fig. 5). Type 1 was the relation of increasing scaling with an obvious inflection point at 990 m. These curves correspond to GYRATE_MN, ED, CONTAG, SHAPE_MN, GM and SHDI. Another type was the relation of decreasing scaling with an inflection point at 990 m. These curves correspond to IJI, CONTIG_MN and UI (Fig. 5(b – d)). The loss of spatial information is caused by an oversized spatial range, and the spatial internal information cannot be reflected to a smaller extent. Therefore, the optimal extent of this study was 990 m.

3.2. *Landscape structure characteristics based on the optimal scale*

3.2.1. *Temporal variation*

The landscape structures of Guiyang City notably changed from 1995 to 2019, and the area distribution of various landscape types was uneven (Fig. 6). Cultivated land and woodland were the dominant landscape types, with their area accounting for more than 72% of the total area.

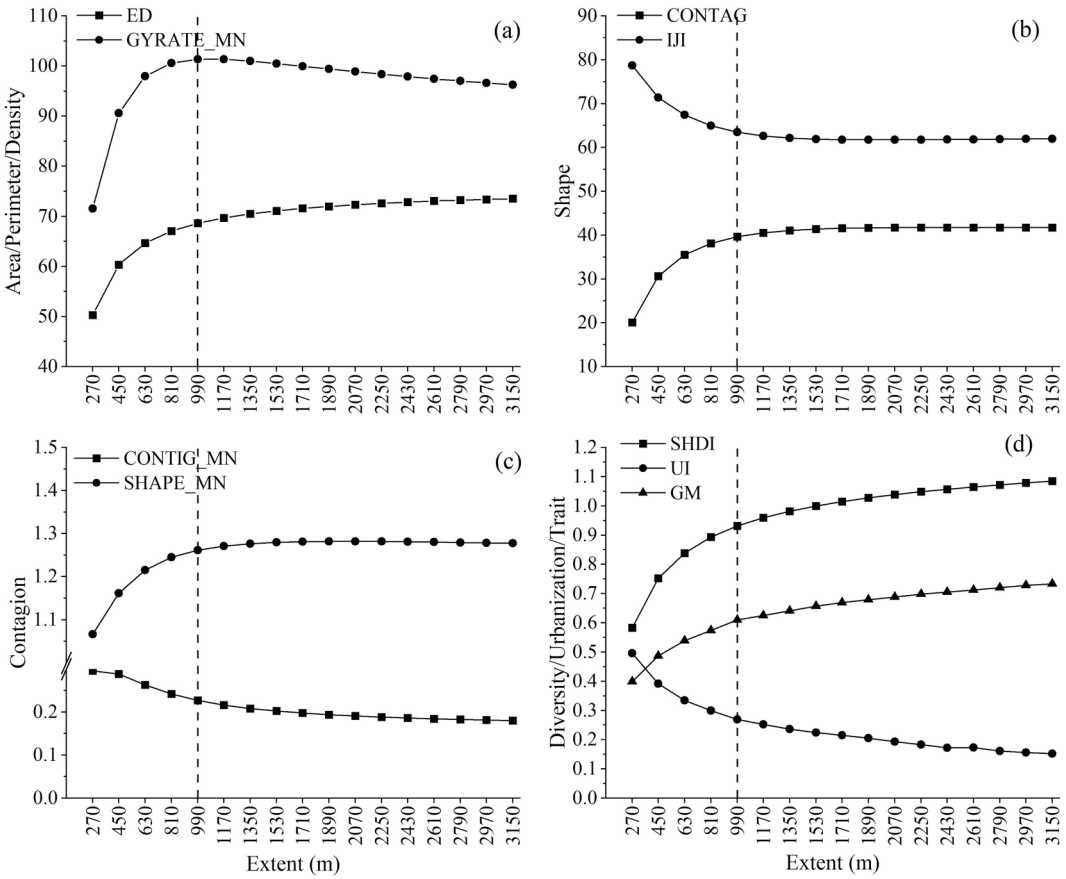

Fig. 5. Landscape indices for various extent sizes ***Notes:*** Edge density (ED); Mean radius of gyration (GYRATE_MN); Contagion index (CONTAG); Interspersion and Juxtaposition index (IJI); Mean contiguity index (CONTIG_MN); Mean shape index (SHAPE_MN); Shannon's diversity index (SHDI); Proportion of urban area (UI); Gibbs-Martin diversity index (GM).

However, the area of woodland and construction land increased significantly, with increment areas of 1282.77 km^2 and 414.26 km^2 and change rates of 16.30% and 5.26%, respectively. In addition, cultivated land, unused land and grassland declined with change rates of 7.98%, 7.32% and 6.18%, respectively (Table 5). This might be related to the occupation of cultivated land due to the growth of population and economy and the implementation of the ecological policy (e.g., the Grain for Green Program). From 1995 to 2019, the landscape types of Guiyang changed dramatically, showing the characteristics of "urbanization and ecologization", which might be related to the increasing area of construction land caused by urbanization and the simultaneous increasing area of woodland due to the implementation of Reforestation Project in 1999 (Chen et al., 2022).

3.2.2. *Spatial variation*

The transformation process between different landscape types was frequent from 1995 to 2019, mainly due to the violent transfer among cultivated land, construction land and woodland (Fig. 6, Fig. 7). The conversion of cultivated land to construction land was drastic with a changed 187.17 km^2 from 2010 to 2015. Spatial distribution displayed obvious directionality, showing a multiaxial distribution pattern with the combination of internal filling and external spread, which might be related to the urban development in two ways: first, in the form of urban continuous development through the growth of previous old city, and second, as a discontinuous expansion in the form of the creation of new clusters in remote areas (Dadashpoor et al., 2019). The area of woodland and construction land expanded synchronously, showing a banded distribution pattern. It showed that in this period from 1995 to 2019, a series of national ecological protection projects and policies have obvious effects on the restoration of forest cover, such as the Pearl river Shelter-belt Project (1996), Reforestation Project (1999) and the construction of forest belt around Guiyang City after 2000 (Chen et al., 2022; Li et al., 2022b). Relying on the unique urban relic mountain resources of karst mountainous cities, a "Forest–Urban" mosaic ecological landscape was formed in the city from outside to inside after 2015.

3.3. *Changes in landscape indices*

3.3.1. *Landscape level*

The values of ED and GM were generally high in the study area, while the value of CONTAG was at a low level, which showed that the fragmentation of the landscape was significant from 1995 to 2019 (Fig. 8). High values of the ED, SHDI and GM in the northwestern part of the study area were gradually spread to the central, northeastern and southern parts, which indicated that the land use structure was diversified. The higher value of SHAPE_MN in the northern and southwestern parts indicated that the landscape complexity increased to a certain extent, which is conducive to the survival of marginal heterogeneous populations and the improvement of biodiversity (Rao et al., 2021). However, the shape of landscape patches was relatively regular, with a value of SHAPE_MN close to 1.0, which was related to urbanization expansion. This urbanization expansion had caused the continuous natural patches to become discontinuous mosaic (Luo et al., 2022). In addition, due to the implementation of a series of ecological restoration measures (especially the Grain for Green Program), cultivated land in the northwestern part had been largely transformed into woodland, which enhanced the landscape connectivity. The spatial distribution

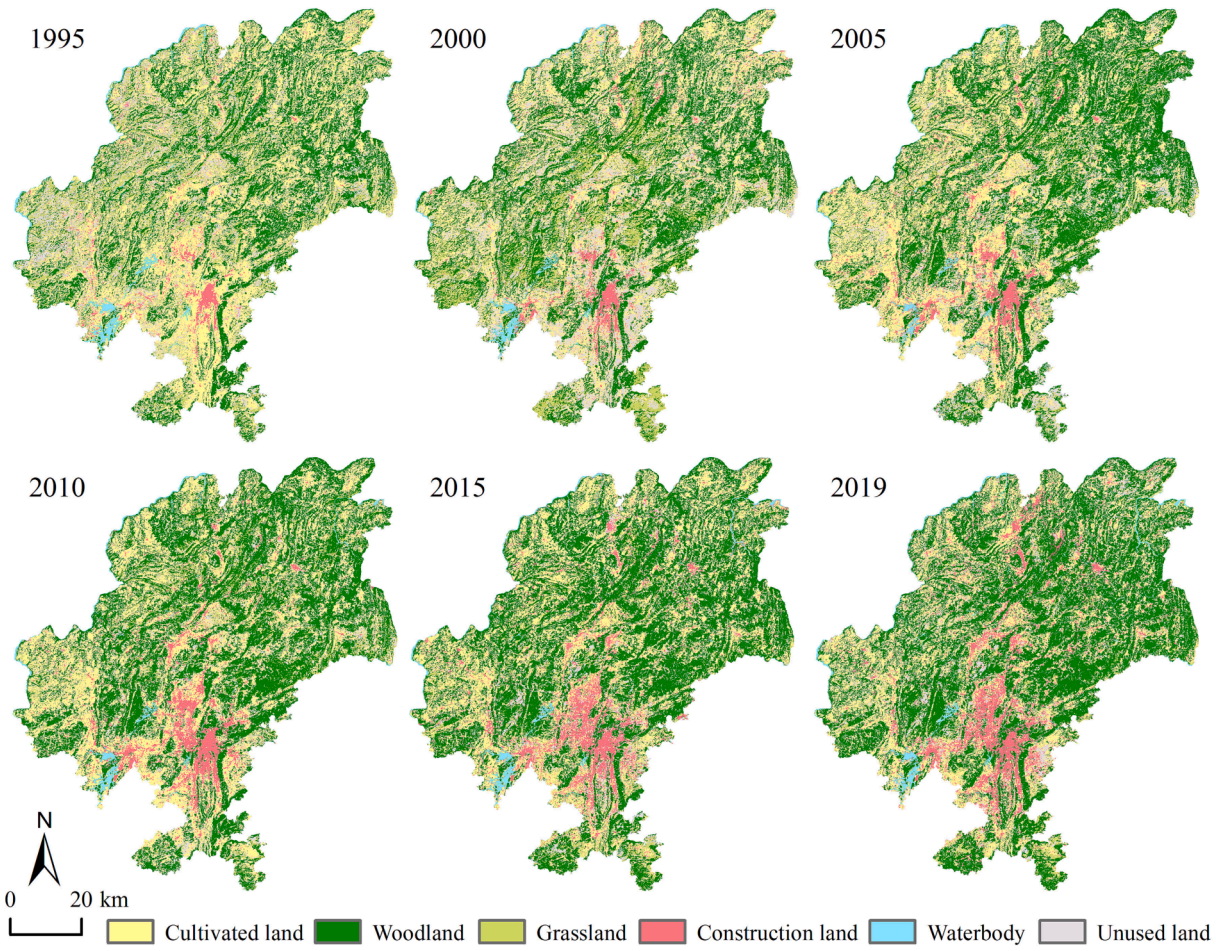

Fig. 6. Spatial distribution map of landscape types.

Table 5
The area (km^2) and ratio (%) of different landscape types from 1995 to 2019.

Land Use Types	1995		2000		2005		2010		2015		2019	
	Area	Ratio	Area	Ratio	Area	Ratio	Area	Ratio	Area	Ratio	Area	Ratio
Cultivated land	3237.98	41.14	3053.34	38.79	2883.03	36.63	2827.63	35.93	2686.80	34.14	2610.22	33.16
Woodland	2462.95	31.29	2819.58	35.82	3170.06	40.28	3409.87	43.32	3597.56	45.71	3745.72	47.59
Grassland	828.78	10.53	709.31	9.01	589.58	7.49	544.68	6.92	522.80	6.64	342.43	4.35
Construction land	149.07	1.89	217.74	2.77	287.03	3.65	373.73	4.75	477.34	6.06	563.33	7.16
Waterbody	138.66	1.76	106.61	1.35	92.63	1.18	102.93	1.31	123.28	1.57	132.09	1.68
Unused land	1053.32	13.38	964.20	12.25	848.43	10.78	611.92	7.77	462.99	5.88	476.98	6.06

characteristics of UI indicated that the urban area was centred on the old city of the study area and spread to other areas, gradually forming the development mode of “multiple group”.

3.3.2. *Class level*

The characteristics of different landscape types were significantly different (Fig. 9). The ED value of cultivated land was the highest, followed by that of woodland, whereas the ED values of construction land and waterbody were low. For the IJI, the value of each landscape type was mainly concentrated between 65% and 80%. This indicated that the areas with serious landscape fragmentation were mainly distributed over cultivated land and woodland, and that the landscape heterogeneity was high. For GYRATE_MN, it increased and then decreased for construction land. Taking the time node in 2010, the expansion mode of urban integration and emerging urban construction was formed successively. Under the guidance of the overall urban planning of Guiyang City (1996–2010) and (2011–2020) approved by the Stats Council since 1990, Guiyang City has entered the stage of rapid development, which had caused the dramatic change in landscape types. For SHAPE_MN, the changes in cultivated land, woodland and construction land were relatively stable. However, the patch shapes of the other landscape types fluctuated due to their smaller areas. In addition, for CONTIG_MN, the value of woodland was significantly larger than other landscape types, which indicated that the proximity between woodland patches was higher than that between other landscape types; however, the connectivity was still poor. This result demonstrated large-scale implementation of a series of ecological protection projects have achieved remarkable results on the restoration of forest cover and environmental protection (Huang et al., 2021; Qiao et al., 2021; Wang et al., 2021a).

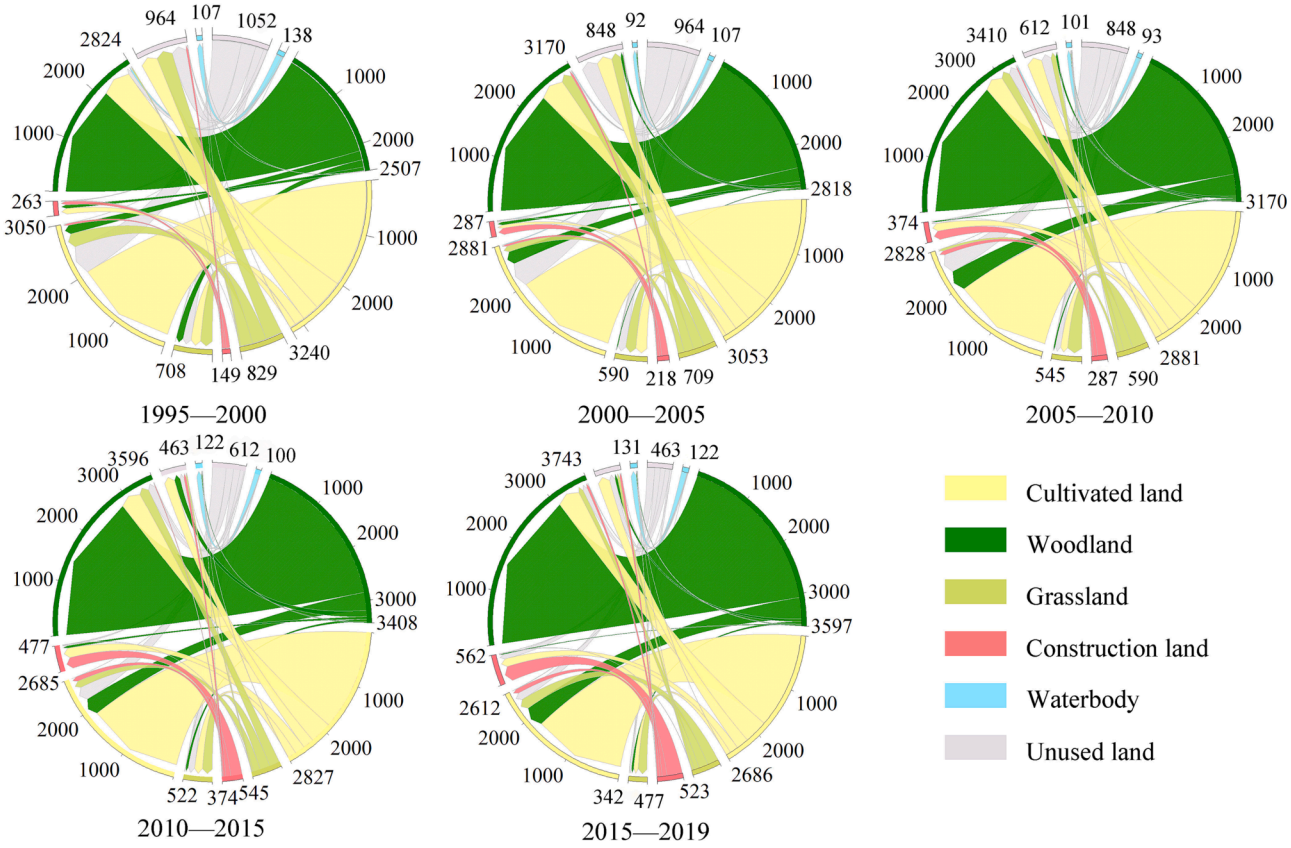

Fig. 7. Landscape type transfer map (km^2).

4. Discussion

4.1. Analysis of accuracy and comparison with other related researches

A landscape index condenses landscape information, which is the general expression of landscape information (Liu et al., 2020). There are significant differences in the ability of different landscape indices to measure landscape pattern characteristics. Therefore, identifying the key landscape indices could assist in understanding the intrinsic relationship between landscape patterns and ecological processes, which is an important basis for ecological protection and planning (Tian, 2020; Zhang et al., 2020). Due to the strong correlation between many indices describing landscape patterns, the direct selection method can easily lead to redundancy among indicators, whereas it is not persuasive to describe landscape patterns with a set of landscape indices that were not independent of each other (Wang et al., 2021c). Correlation analysis and principal component analysis are used to determine the optimal landscape indices, which has been verified, and the results have been demonstrated to be reliable (Toosi et al., 2022; Topaloğlu et al., 2021). Herein, a principal component analysis was used to determine the optimal landscape indices, we found that the optimal landscape indices were ED, GYRATE_MN, CONTIG_MN, SHAPE_MN, CONTAG, IJI, SHDI, GM and UI (Table 4). This was not completely consistent with landscape indices selected by previous landscape pattern analysis in the same latitude and other karst mountainous regions, which might be related to different study purposes and study areas (Table 6). Several studies usually consider the various study objects and focused on selecting relevant landscape indices by evaluating the response of landscape indices for changes in specific landscape types (Guo et al., 2021; Qin et al., 2022; Toosi et al., 2022). At the same latitude (Miami metropolitan area and Dongting Lake Basin), the spatial heterogeneity of the study area may also lead to inconsistent results (Ning and Ouyang, 2023; Rifat and Liu, 2019). In addition, most studies have mainly based their methods on the established empirical choices of others, which may be one of the reasons for the different results (Barwicka and Milecka, 2021; Li et al., 2019).

The characteristics of landscape patterns are significantly different with the change of scales. The optimal landscape scale can be used to not only accurately explore spatiotemporal variation characteristics of landscape patterns, but also to scientifically disclose variation laws of ecological structures and functions of landscapes (Tian et al., 2019). On the premise of optimal indices in this study, the optimal scale was determined based on the selection of optimal landscape indices using qualitative and quantitative methods. These methods have been widely verified in Fujian, Shanghai, the Three Gorges Reservoir, and other places (Ai et al., 2022; Guan et al., 2022; Wang et al., 2021b; Zhang et al., 2020). We found that the most appropriate grain and extent in Guiyang City were 90 m and 1000 m, respectively (Fig. 5). These are distinct from the results of studies in other regions of the same latitude and abroad, which may be affected by the resolution of basic data and the study area (Table 7). For one thing, the resolution of a remote sensing image is a significant parameter underlying scale, which affects the determination of the optimal landscape scale (Alhamad et al., 2011). If the accuracy of basic data is higher, then the optimal scale is always smaller (Ai et al., 2022; Campagnaro et al., 2017; Hu et al., 2022; Pham et al., 2021). For another, the differences in the driving factors for changes in regional landscape patterns and the study area will lead to differences in the optimal scale (Ren et al., 2018; Wang and Li, 2021; Wang et al., 2021b; Xu et al., 2020). In addition, to determine the optimal landscape extent, previous research proposed an alternative approach where the sample unit should be 2 to 5 times larger than the landscape grain to avoid bias (Farina, 2022). However, the result of this study was 8.3 times larger than the average patch area, which was larger than the result calculated using the previous method. This difference

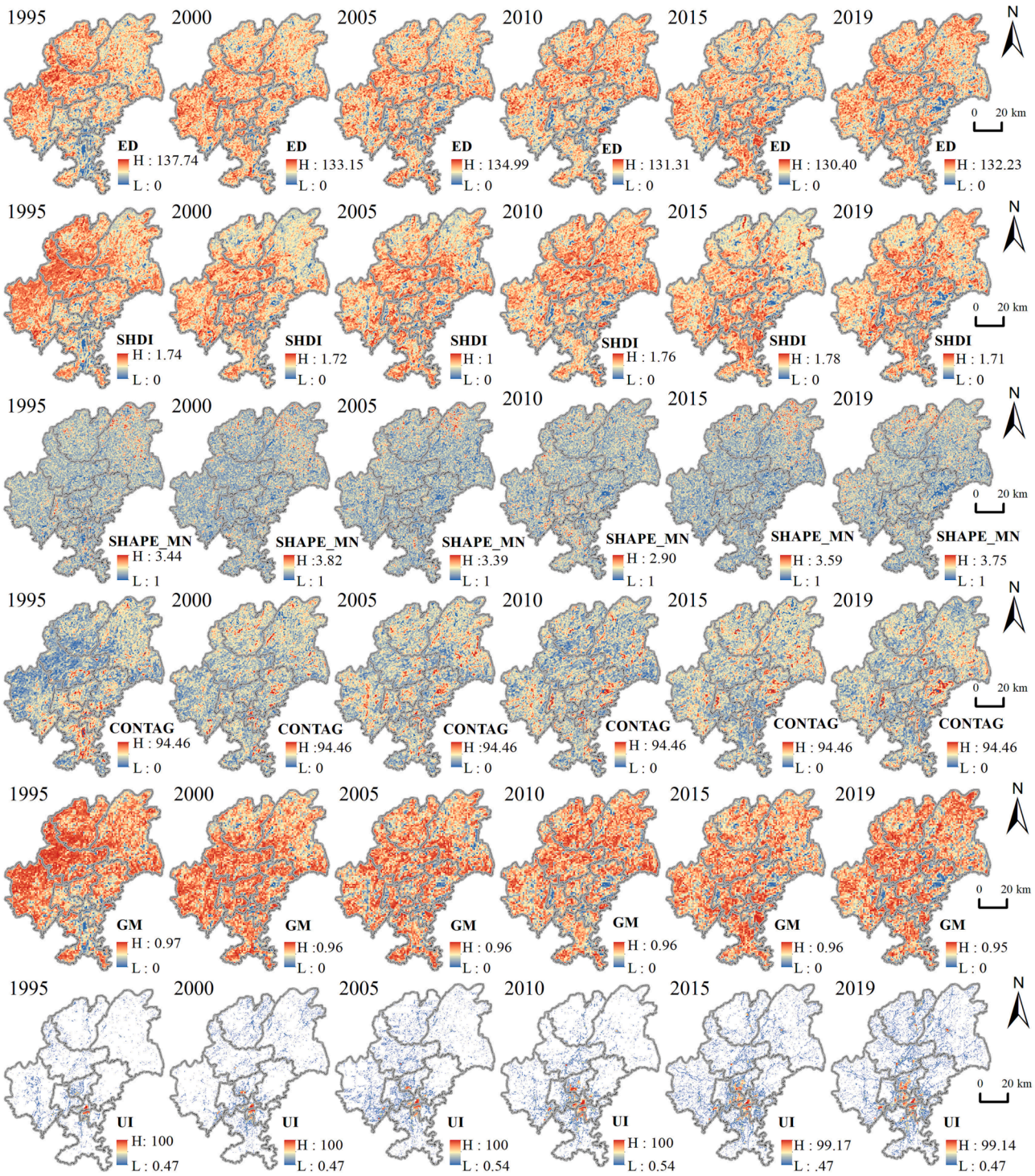

Fig. 8. Spatial distribution of landscape indices from 1995 to 2019 at landscape level ***Notes:*** Edge density (ED); Shannon's diversity index (SHDI); Mean shape index (SHAPE_MN); Contagion index (CONTAG); Gibbs-Martin diversity index (GM); Proportion of urban area (UI).

might be attributed to the fragmentation of the terrain. Some landscapes are divided into a large number of small patches because of the particular physiognomy in karst regions, resulting in large landscape fragmentation and a small average patch area (Fig. 8). Here, in this study, the optimal scale reduces the error caused by scale dependence and compensates for the deficiency in the research of extent in karst mountain cities, which is helpful to understand the internal relationship between landscape pattern and ecological process, and provide a series of sustainable ecological planning and protection decisions.

4.2. *Changes of landscape patterns*

With global development and rapid urbanization, human activities and natural drivers affect landscape patterns which in turn influence biodiversity and ecosystem function, which further impact ecosystem services and human wellbeing (Gong et al., 2021; Wu, 2021). In this study, the area of construction land in Guiyang City increased from 149.07 km^2 in 1995 to 563.33 km^2 in 2019, with a tendency of clearly decreasing cultivated land (Table 5). This finding is consistent with the results of the relevant study (Luo et al., 2022). Urban expansion caused

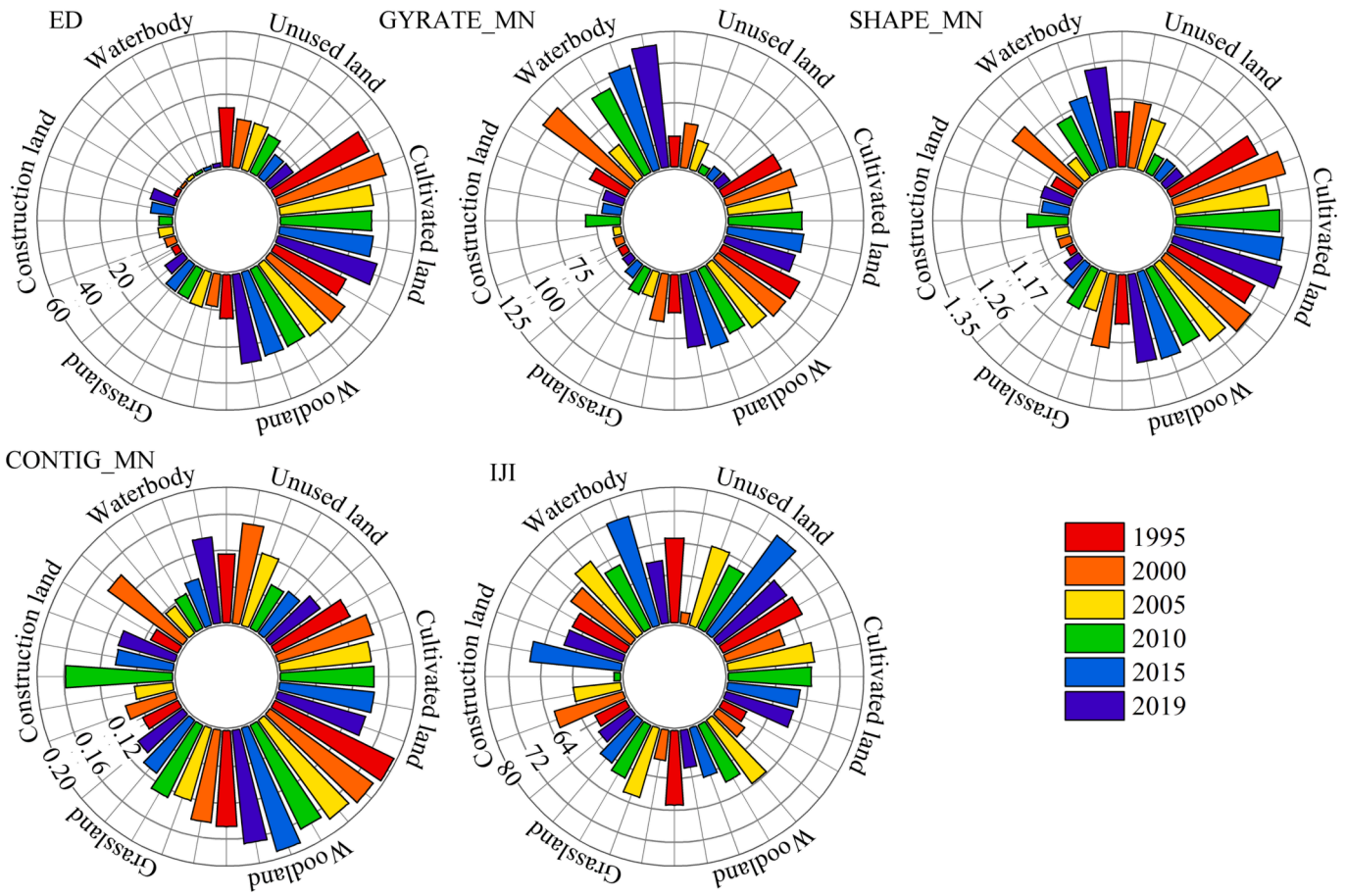

Fig. 9. Landscape indices from 1995 to 2019 at class level ***Notes:*** Edge density (ED); Mean radius of gyration (GYRATE_MN); Mean shape index (SHAPE_MN); Mean contiguity index (CONTIG_MN); Interspersion and Juxtaposition index (IJI).

Table 6
Comparison with the results of other scholars.

Study area	Landscape indices	Date Sources
Karst region in Sichuan Basin	NP、LSI、CONTAG、MESH	(Guo et al., 2021)
Persian Gulf in southern Iran	TE、PD、SPLIT、CONTAG、SHDI, et al.	(Toosi et al., 2022)
Liuzhou city in Guangxi Zhuang Autonomous Region	NP、LSI、SPLIT、CONTAG、AI、SHDI、SHEI	(Qin et al., 2022)
Miami Metropolitan Area	NP、LPI、LSI、SHAPE_AM	(Rifat and Liu, 2019)
Dongting Lake Basin	FRAC、CONTAG、SHDI、SHEI、IJI	(Ning and Ouyang, 2023)

by human activities is an important factor in landscape pattern change. Urbanization is an important engine of modernization and economic growth, which can promote regional economic and social development, but also caused dramatic changes in landscape patterns (Hong et al., 2021). Driven by population factors, construction land is mainly increased by encroaching on cultivated land and ecological land (such as woodland and grassland) (Luo et al., 2022). In addition, the spatial distribution characteristics of construction land and woodland types are obvious and a "Forest-Urban" mosaic ecological landscape was formed in the city from outside to inside (Fig. 6, Fig. 7). It might be influenced by urban planning and land use policy. Woodland gradually becomes the dominated landscape type in the study area, with a tendency of clearly increasing (Table 5, Fig. 6). This finding is consistent with the results of relevant studies (Luo et al., 2022; Wang et al., 2022). This is mainly benefited by the large-scale implementation of a series of ecological protection projects (such as the Grain for Green Program, closed hillside

Table 7
Comparison of different research results.

Study area	Area (km^2)	Data types	Grain (m)	Extent (m)	Date Sources
Anshun in Guizhou	300.54	Pleiades satellite images	20	–	(Ren et al., 2018)
Haitan Island in Fujian	324.88	Landsat satellite images	75	–	(Ai et al., 2022)
Nanchang in Jiangxi	7195.00	Landsat satellite images	30	–	(Wang and Li, 2021)
Shanghai	6340.00	Landsat satellite images	60	–	(Wang et al., 2021b)
Jordan	2500.00	Landsat satellite images	85.5–256.5	–	(Alhamad et al., 2011)
Conterminous United States	8,059,023.00	National Land Cover Database	9930	–	(Xu et al., 2020)
Tovanella	10.40	Aerial photos	–	200–400	(Campagnaro et al., 2017)
The Complex of Huế Monuments	218.00	SPOT imagery data	–	550	(Pham et al., 2021)
Haitan Island in Fujian	324.88	Landsat satellite images	–	1050	(Ai et al., 2022)
Fuzhou in Fujian	11,968.00	Landsat satellite images	–	3000	(Hu et al., 2022)

afforestation and the Karst Rocky Desertification Restoration Project) (Huang et al., 2021; Qiao et al., 2021; Wang et al., 2021a). These projects have greatly promoted the restoration of vegetation and improved the karst ecological environment. In addition, industrial structure is also an important factor to promote the dramatic change of landscape patterns in Guiyang (Luo et al., 2022).

Different landscape pattern index could reflect different characteristics in landscape patterns. In the study, the characteristics of high overall landscape fragmentation, diversity and low landscape connectivity, and urban expansion were reflected by ED, GM, CONTAG, and UI (Fig. 8, Fig. 9). This result also agrees with the finding of Lu et al. (2021). As a mountain city, urban expansion in Guiyang City was limited and affected by geographic factors and government policies (Liao et al., 2022). On the one hand, areas with low-lying terrain and flat topography are conductive to human activities, which determines the basis of the landscape fragmentation, especially in karst areas with special geological conditions (Luo et al., 2022). On the other hand, the change in the land use structure was caused by urbanization expansion, which caused the continuous natural patches to become discontinuous mosaic (Luo et al., 2022). This is the main reason for low landscape connectivity, which may lead to the loss of animal and plant habitats, thus bringing adverse effects on human sustainable development (Dadashpoor et al., 2019). However, urban sprawl can also be beneficial and urbanization sometimes increases species richness. For example, Boscutti et al. (2022) showed that both increasing urban cover and patch shape complexity contributed to increase the number of exotic species. SHAPE_MN reflected the regular shape of the landscape (Fig. 8). The infrastructure construction in mountainous cities with complex terrain usually costs more in funds and materials than with higher technical requirements than that in plain cities, which could also contribute to the simpler patch shape in Guiyang City (He et al., 2022; Jia et al., 2020). In addition, due to the ecological barrier with woodland as the advantage, which has been actively built in Guiyang City, through the continuous construction of forest belts around the city, eminent connectivity has been gradually formed between woodland patches (Fig. 9). Some studies have shown that negative impacts on biodiversity often result from the decrease in habitat connectivity and ecosystem integrity and the aggravation of edge effects (Li et al., 2022a). Therefore, unreasonable urban planning and improved ecosystem landscape planning should be corrected to promote healthy urban development and urban ecological sustainability. In doing this, first, the laws of nature need to be respected to maintain the integrity of the landscape of the natural landscape, such as forests and rivers, as much as possible. Second, dynamically managed to ensure the rational and orderly development of landscape structure. In addition, we should pay attention to the construction between urban ecological patches and enhance the connectivity between patches in areas with obvious urban expansion and promote compact urban patterns by connecting the natural corridors on both sides of the urban road (Li et al., 2022a).

4.3. Uncertainty analysis and future outlook

In this study, optimal landscape indices and scales were determined, which enhanced the accuracy of landscape patterns analysis in the karst mountainous region and effectively and revealed the characteristics of landscape pattern in the process of rapid urbanization. However, our research still has certain uncertainties and limitations. The Landsat satellite data used in this study have a medium-resolution of 30 m. However, the main limitation of using landscape pattern indices is that its sensitivity to quantifying urban form largely depends on the accuracy of land use classification (Liu et al., 2021; Taubenböck et al., 2019). To retrieve information about the characteristics and mechanisms of landscape pattern changes at a finer scale, high spatial resolution imagery such as QuickBird and Lidar could be used in the future. In addition, traditional two-dimensional landscape indices were selected in the study of landscape scale effect, which focused on statistical surface morphology (Ge et al., 2021; Wu et al., 2017). Two-dimensional landscape indices could not express the spatial heterogeneity of complex three-dimensional structures, especially for mountainous cities (Kong et al., 2022). The development of urban areas is not only reflected in the horizontal direction, but also has great changes in the vertical direction. The three-dimensional features of urban areas can be more intuitively reflected by landscape indices calculated based on the average height, height standard deviation and floor area ratio of buildings (Canedoli et al., 2022; Liu et al., 2017). Thus, future studies consider that three-dimensional indices suitable for the study area should be constructed to analyze landscape pattern characteristics more intuitively and comprehensively. In addition, the tools are commonly used for identifying the scale mainly include spatial statistics, landscape indices methods and fractal dimension analysis (Gustafson, 2019). The landscape pattern indices method, as one of the research methods to study the impact of scale effect on landscape pattern analysis, has been widely used in landscape ecology (Alhamad et al., 2011). Landscape pattern index method can only analyze landscape pattern at a single scale, and many landscape pattern indices are sensitive to the boundary of the study area (Deng et al., 2022). There, future studies should explore the scale effect in multiple dimensions to better reveal the relationship between landscape patterns and ecological processes.

5. Conclusion

We concluded that nine landscape indices (i.e., ED, GYRATE_MN, CONTIG_MN, SHAPE_MN, CONTAG, IJI, SHDI, UI and GM) were identified as the optimal landscape index for analyzing the landscape pattern in Guiyang City, with the optimal landscape grain and extent of 90 m and 1000 m, respectively. Woodland and cultivated land were the predominant landscape types during the study periods. However, the landscape structure in Guiyang City from 1995 to 2019 was dramatically changed with the constantly increment of woodland and construction land, urbanization and ecologization were main trends of landscape pattern changes. In addition, due to the implementation of a series of ecological restoration measures, the continuity of the spatial distribution of the woodland always remained at a high level. Furthermore, the landscape pattern in Guiyang City is still facing severe challenges for the intensification of landscape fragmentation and regularization of patch shape. The findings of this study can provide guidance and a reference for landscape pattern planning at different development stages in karst mountainous regions.

Declaration of Competing Interest

The authors declare that they have no known competing financial interests or personal relationships that could have appeared to influence the work reported in this paper.

Data availability

Data will be made available on request.

Acknowledgments

This work was supported by the National Nature Science Foundation of China (NSFC) project (Grant numbers 42061039 and 41701319); the Cultivation Project of Guizhou University, grant number (2020)46 and the Construction Program of Biology First-class Discipline in Guizhou, grant number GNYL (2017)009.

References

Abbas, Z., Zhu, Z., Zhao, Y., 2022. Spatiotemporal analysis of landscape pattern and structure in the Greater Bay Area. China. Earth Sci. Inf. 1–16 https://doi.org/10.1007/s12145-022-00782-y.

Ai, J., Yu, K., Zeng, Z., Yang, L., Liu, Y., Liu, J., 2022. Assessing the dynamic landscape ecological risk and its driving forces in an island city based on optimal spatial scales: Haitan Island. China. Ecol. Indic. 137, 108771 https://doi.org/10.1016/j.ecolind.2022.108771.

Alhamad, M.N., Alrababah, M.A., Feagin, R.A., Gharaibeh, A., 2011. Mediterranean drylands: the effect of grain size and domain of scale on landscape metrics. Ecol. Indic. 11, 611–621. https://doi.org/10.1016/j.ecolind.2010.08.007.

Bai, X., Zhang, S., Li, C., Xiong, L., Song, F., Du, C., Li, M., Luo, Q., Xue, Y., Wang, S., 2023. A carbon neutrality capacity index for evaluating carbon sink contributions. Environ. Sci. Ecotechnol. 100237 https://doi.org/10.1016/j.ese.2023.100237.

Barwicka, S., Milecka, M., 2021. The Use of Selected Landscape Metrics to Evaluate the Transformation of the Rural Landscape as a Result of the Development of the Mining Function—A Case Study of the Puchaczów Commune. Sustainability 13, 12279. https://doi.org/10.3390/su132112279.

Boscutti, F., Lami, F., Pellegrini, E., Buccheri, M., Busato, F., Martini, F., Sibella, R., Sigura, M., Marini, L., 2022. Urban sprawl facilitates invasions of exotic plants across multiple spatial scales. Biol. Invasions 24, 1497–1510. https://doi.org/10.1007/s10530-022-02733-6.

Campagnaro, T., Frate, L., Carranza, M.L., Sitzia, T., 2017. Multi-scale analysis of alpine landscapes with different intensities of abandonment reveals similar spatial pattern changes: Implications for habitat conservation. Ecol. Indic. 74, 147–159. https://doi.org/10.1016/j.ecolind.2016.11.017.

Canedoli, C., Ficetola, G.F., Corengia, D., Tognini, P., Ferrario, A., Padoa-Schioppa, E., 2022. Integrating landscape ecology and the assessment of ecosystem services in the study of karst areas. Landsc. Ecol. 1–19 https://doi.org/10.1007/s10980-021-01351-2.

Chen, F., Bai, X., Liu, F., Luo, G., Tian, Y., Qin, L., Li, Y., Xu, Y., Wang, J., Wu, L., 2022. Analysis long-term and spatial changes of forest cover in typical karst areas of China. Land 11, 1349. https://doi.org/10.3390/land11081349.

Chen, X., Wang, Z., Bao, Y., 2021b. Cool island effects of urban remnant natural mountains for cooling communities: A case study of Guiyang. China. Sustainable Cities Soc. 71, 102983 https://doi.org/10.1016/j.scs.2021.102983.

Chen, Q., Xiong, K., Zhao, R., 2021a. Assessment on erosion risk based on GIS in typical Karst region of Southwest China. Eur. J. Remote Sens. 54, 405–416. https://doi.org/10.1080/22797254.2020.1793688.

Cheung, A.K.L., Brierley, G., O'Sullivan, D., 2016. Landscape structure and dynamics on the Qinghai-Tibetan Plateau. Ecol. Model. 339, 7–22. https://doi.org/10.1016/j.ecolmodel.2016.07.015.

Cushman, S.A., Gutzweiler, K., Evans, J.S., McGarigal, K., 2010. The gradient paradigm: a conceptual and analytical framework for landscape ecology, Spatial complexity, informatics, and wildlife conservation. Springer, pp. 83-108. 10.1007/978-4-431-87771-4.

Dadashpoor, H., Azizi, P., Moghadasi, M., 2019. Land use change, urbanization, and change in landscape pattern in a metropolitan area. Sci. Total Environ. 655, 707–719. https://doi.org/10.1016/j.scitotenv.2018.11.267.

Dadashpoor, H., Salarian, F., 2020. Urban sprawl on natural lands: Analyzing and predicting the trend of land use changes and sprawl in Mazandaran city region. Iran. Environment, Development and Sustainability 22, 593–614. https://doi.org/10.1007/s10668-018-0211-2.

Dai, L., Wang, Z., 2023. Construction and optimization strategy of ecological security pattern based on ecosystem services and landscape connectivity: a case study of Guizhou Province. China. Environ. Sci. Pollut. Res. 1–17 https://doi.org/10.1007/s11356-023-25417-7.

Deng, L., Zhang, Q., Cheng, Y., Cao, Q., Wang, Z., Wu, Q., Qiao, J., 2022. Underlying the influencing factors behind the heterogeneous change of urban landscape patterns since 1990: A multiple dimension analysis. Ecol. Indic. 140, 108967 https://doi.org/10.1016/j.ecolind.2022.108967.

Fang, S., Zhao, Y., Han, L., Ma, C., 2017. Analysis of Landscape Patterns of Arid Valleys in China. Based on Grain Size Effect. Sustainability 9, 2263. https://doi.org/10.3390/su9122263.

Farina, A., 2022. Scaling Patterns and Processes Across Landscapes. In: Farina, A. (Ed.), Principles and Methods in Landscape Ecology: An Agenda for the Second Millennium. Springer International Publishing, Cham, pp. 157–176. https://doi.org/10.1007/978-3-030-96611-9_4.

Fu, B., Liang, D., Lu, N., 2011. Landscape ecology: Coupling of pattern, process, and scale. Chin Geogr Sci. 21, 385–391. https://doi.org/10.1007/s11769-011-0480-2.

Fu, G., Wang, W., Li, J., Xiao, N., Qi, Y., 2021. Prediction and Selection of Appropriate Landscape Metrics and Optimal Scale Ranges Based on Multi-Scale Interaction Analysis. Land 10, 1192. https://doi.org/10.3390/land10111192.

Ge, M., Fang, S., Gong, Y., Tao, P., Yang, G., Gong, W., 2021. Understanding the correlation between landscape pattern and vertical urban volume by time-series remote sensing data: A case study of Melbourne. ISPRS Int. J. Geo-Inf. 10, 14. https://doi.org/10.3390/ijgi10010014.

Gong, S., Wang, S., Bai, X., Luo, G., Wu, L., Chen, F., Qian, Q., Xiao, J., Zeng, C., 2021. Response of the weathering carbon sink in terrestrial rocks to climate variables and ecological restoration in China. Sci. Total Environ. 750, 141525 https://doi.org/10.1016/j.scitotenv.2020.141525.

Guan, D., Jiang, Y., Cheng, L., 2022. How can the landscape ecological security pattern be quantitatively optimized and effectively evaluated? An integrated analysis with the granularity inverse method and landscape indicators. Environ. Sci. Pollut. Res. 29, 41590–41616. https://doi.org/10.1007/s11356-021-16759-1.

Guo, Y., Du, X., Chen, H., Zheng, G., Zhang, X., Wang, Q., 2021. Influence of shale gas development on core forests in the subtropical karst region in southwestern China. Sci. Total Environ. 771, 145287 https://doi.org/10.1016/j.scitotenv.2021.145287.

Gustafson, E.J., 2019. How has the state-of-the-art for quantification of landscape pattern advanced in the twenty-first century? Landsc. Ecol. 34, 2065–2072. https://doi.org/10.1007/s10980-018-0709-x.

He, Y., Sherbinin, A.d., Shi, G., Xia, H., 2022. The Economic Spatial Structure Evolution of Urban Agglomeration under the Impact of High-Speed Rail Construction: Is There a Difference between Developed and Developing Regions? Land 11, 1551. https://doi.org/10.3390/land11091551.

Hong, T., Yu, N., Mao, Z., Zhang, S., 2021. Government-driven urbanisation and its impact on regional economic growth in China. Cities 117, 103299. https://doi.org/10.1016/j.cities.2021.103299.

Hu, Z., Wang, S., Bai, X., Luo, G., Li, Q., Wu, L., Yang, Y., Tian, S., Li, C., Deng, Y., 2020. Changes in ecosystem service values in karst areas of China. Agric. Ecosyst. Environ. 301, 107026 https://doi.org/10.1016/j.agee.2020.107026.

Hu, X., Xu, C., Chen, J., Lin, Y., Lin, S., Wu, Z., Qiu, R., 2022. A Synthetic Landscape Metric to Evaluate Urban Vegetation Quality: A Case of Fuzhou City in China. Forests 13, 1002. https://doi.org/10.3390/f13071002.

Huang, J., Ge, Z., Huang, Y., Tang, X., Shi, Z., Lai, P., Song, Z., Hao, B., Yang, H., Ma, M., 2021. Climate change and ecological engineering jointly induced vegetation greening in global karst regions from 2001 to 2020. Plant Soil 1–20. https://doi.org/10.1007/s11104-021-05054-0.

Jia, L., Ma, Q., Du, C., Hu, G., Shang, C., 2020. Rapid urbanization in a mountainous landscape: patterns, drivers, and planning implications. Landsc. Ecol. 35, 2449–2469. https://doi.org/10.1007/s10980-020-01056-y.

Jia, Y., Tang, L., Xu, M., Yang, X., 2019. Landscape pattern indices for evaluating urban spatial morphology–A case study of Chinese cities. Ecol. Indic. 99, 27–37. https://doi.org/10.1016/j.ecolind.2018.12.007.

Kong, F., Chen, J., Middel, A., Yin, H., Li, M., Sun, T., Zhang, N., Huang, J., Liu, H., Zhou, K., Ma, J., 2022. Impact of 3-D urban landscape patterns on the outdoor thermal environment: A modelling study with SOLWEIG. Comput. Environ. Urban Syst. 94, 101773 https://doi.org/10.1016/j.compenvurbsys.2022.101773.

Křováková, K., Semerádová, S., Mudrochová, M., Skaloš, J., 2015. Landscape functions and their change–a review on methodological approaches. Ecol. Eng. 75, 378–383. https://doi.org/10.1016/j.ecoleng.2014.12.011.

Kupfer, J.A., 2012. Landscape ecology and biogeography. Prog. Phys. Geogr.: Earth Environ. 36, 400–420. https://doi.org/10.1177/0309133309501900102.

Lausch, A., Blaschke, T., Haase, D., Herzog, F., Syrbe, R.-U., Tischendorf, L., Walz, U., 2015. Understanding and quantifying landscape structure–A review on relevant process characteristics, data models and landscape metrics. Ecol. Model. 295, 31–41. https://doi.org/10.1016/j.ecolmodel.2014.08.018.

Li, G., Fang, C., Li, Y., Wang, Z., Sun, S., He, S., Qi, W., Bao, C., Ma, H., Fan, Y., 2022a. Global impacts of future urban expansion on terrestrial vertebrate diversity. Nat. Commun. 13, 1–12. https://doi.org/10.1038/s41467-022-29324-2.

Li, H., Peng, J., Yanxu, L., Yi'na, H., 2017. Urbanization impact on landscape patterns in Beijing City, China: A spatial heterogeneity perspective. Ecol. Indic. 82, 50–60. https://doi.org/10.1016/j.ecolind.2017.06.032.

Li, Z., Shi, T., Wu, Y., Zhang, H., Juan, Y.-H., Ming, T., Zhou, N., 2020. Effect of traffic tidal flow on pollutant dispersion in various street canyons and corresponding mitigation strategies. Energy Built Environ. 1, 242–253. https://doi.org/10.1016/j.enbenv.2020.02.002.

Li, J., Wei, Y., Li, Y., 2022b. Dynamic evaluation and simulation of land carrying capacity in a karst mountainous area—a case study of Guiyang. Arabian J. Geosci. 15, 1–21. https://doi.org/10.1007/s12517-022-09810-z.

Li, H., Wu, J., 2004. Use and misuse of landscape indices. Landsc. Ecol. 19, 389–399. https://doi.org/10.1023/B:LAND.0000030441.15628.d6.

Li, Y., Li, Y., Fan, P., Long, H., 2019. Impacts of land consolidation on rural human–environment system in typical watershed of the Loess Plateau and implications for rural development policy. Land Use Policy 86, 339–350. https://doi.org/10.1016/j.landusepol.2019.04.026.

Liao, S., Cai, H., Tian, P., Zhang, B., Li, Y., 2022. Combined impacts of the abnormal and urban heat island effect in Guiyang, a typical Karst Mountain City in China. Urban Clim. 41, 101014 https://doi.org/10.1016/j.uclim.2021.101014.

Liu, M., Bai, X., Tan, Q., Luo, G., Zhao, C., Wu, L., Luo, X., Ran, C., Zhang, S., 2022a. Climate Change Enhances the Positive Contribution of Human Activities to Vegetation restoration in China. Geocarto Int. 1–24 https://doi.org/10.1080/10106049.2022.2082542.

Liu, Y., Chen, C., Li, J., Chen, W., 2020. Characterizing three dimensional (3-D) morphology of residential buildings by landscape metrics. Landsc. Ecol. 35, 2587–2599. https://doi.org/10.1007/s10980-020-01084-8.

Liu, M., Hu, Y., Li, C., 2017. Landscape metrics for three-dimensional urban building pattern recognition. Appl. Geogr. 87, 66–72. https://doi.org/10.1016/j.apgeog.2017.07.011.

Liu, H., Huang, B., Zhan, Q., Gao, S., Li, R., Fan, Z., 2021. The influence of urban form on surface urban heat island and its planning implications: Evidence from 1288 urban clusters in China. Sustainable Cities Soc. 71, 102987 https://doi.org/10.1016/j.scs.2021.102987.

Liu, S., Wang, Z., Wu, W., Yu, L., 2022b. Effects of landscape pattern change on ecosystem services and its interactions in karst cities: A case study of Guiyang City in China. Ecol. Indic. 145, 109646 https://doi.org/10.1016/j.ecolind.2022.109646.

Liu, Y., Wang, S., Chen, Z., Tu, S., 2022c. Research on the Response of Ecosystem Service Function to Landscape Pattern Changes Caused by Land Use Transition: A Case Study of the Guangxi Zhuang Autonomous Region. China. Land 11, 752. https://doi.org/10.3390/land11050752.

Lu, Q., Zhao, C., Wang, J., 2021. Landscape Fragmentation Evolution in Karst Mountainous Area Based on Terrain Gradient – A Case Study of Guiyang City. Res Soil Water Conserv. 28, 242–248. https://doi.org/10.13869/j.cnki.rswc.20201221.001.

Luo, Y., Wang, Z., Zhou, X., Hu, C., Li, J., 2022. Spatial-Temporal Driving Factors of Urban Landscape Changes in the Karst Mountainous Regions of Southwest China: A Case Study in Central Urban Area of Guiyang City. Sustainability 14, 8274. https://doi.org/10.3390/su14148274.

Maity, B., Mallick, S.K., Rudra, S., 2021. Integration of urban expansion with hybrid road transport network development within Haldia Municipality. West Bengal. EGYPT J REMOTE SENS. 24, 471–483. https://doi.org/10.1016/j.ejrs.2020.10.005.

Migenda, N., Möller, R., Schenck, W., 2021. Adaptive dimensionality reduction for neural network-based online principal component analysis. PLoS ONE 16, e0248896. https://doi.org/10.1371/journal.pone.0248896.

Mohamed, A., Worku, H., Kindu, M., 2021. Quantification and mapping of the spatial landscape pattern and its planning and management implications a case study in Addis Ababa and the surrounding area. Ethiopia. Geol. Ecol. Landscapes 5, 161–172. https://doi.org/10.1080/24749508.2019.1701309.

Ning, Q., Ouyang, X., 2023. Spatio-temporal characteristics and mechanism of ecological degradation in a hilly southern area—a case study of Dongting Lake Basin. Environ. Sci. Pollut. Res. 1–11. https://doi.org/10.1007/s11356-023-25514-7.

Peng, J., Liu, Y., Wu, J., Lv, H., Hu, X., 2015. Linking ecosystem services and landscape patterns to assess urban ecosystem health: A case study in Shenzhen City. China. Landsc. Urban Plann. 143, 56–68. https://doi.org/10.1016/j.landurbplan.2015.06.007.

Pham, V.M., Van Nghiem, S., Van Pham, C., Luu, M.P.T., Bui, Q.T, 2021. Urbanization impact on landscape patterns in cultural heritage preservation sites: a case study of the complex of Huế Monuments. Vietnam. Landsc. Ecol. 36, 1235–1260. https://doi.org/10.1007/s10980-020-01189-0.

Qiao, Y., Jiang, Y., Zhang, C., 2021. Contribution of karst ecological restoration engineering to vegetation greening in southwest China during recent decade. Ecol. Indic. 121, 107081 https://doi.org/10.1016/j.ecolind.2020.107081.

Qin, F., Fukamachi, K., Shibata, S., 2022. Land-Use/Landscape Pattern Changes and Related Environmental Driving Forces in a Dong Ethnic Minority Village in Southwestern China. Land 11, 349. https://doi.org/10.3390/land11030349.

Rao, Y., Dai, J., Dai, D., He, Q., Wang, H., 2021. Effect of Compactness of Urban Growth on Regional Landscape Ecological Security. Land 10, 848. https://doi.org/10.3390/land10080848.

Ren, M., Wang, Z., Wang, Z., Zeng, Y., He, L., 2018. Grain size effect of karst mountainous urban landscape pattern indices in the central Guizhou: A case study of Anshun City. Chinese. J. Ecol. 37, 272–280. https://doi.org/10.13292/j.1000-4890.201810.038.

Rifat, S.A.A., Liu, W., 2019. Quantifying spatiotemporal patterns and major explanatory factors of urban expansion in Miami Metropolitan Area during 1992–2016. Remote Sens. 11, 2493. https://doi.org/10.3390/rs11212493.

Song, F., Wang, S., Bai, X., Wu, L., Wang, J., Li, C., Chen, H., Luo, X., Xi, H., Zhang, S., 2022. A new indicator for global food security assessment: harvested area rather than cropland area. Chin Geogr Sci. 32, 204–217. https://doi.org/10.1007/s11769-022-1264-6.

Taubenböck, H., Wurm, M., Geiß, C., Dech, S., Siedentop, S., 2019. Urbanization between compactness and dispersion: designing a spatial model for measuring 2D binary settlement landscape configurations. Int. J. Digital Earth 12, 679–698. https://doi.org/10.1080/17538947.2018.1474957.

Tian, Y., 2020. Mapping suburbs based on spatial interactions and effect analysis on ecological landscape change: A case study of Jiangsu Province from 1998 to 2018. Eastern China. Land 9, 159. https://doi.org/10.3390/land9050159.

Tian, P., Cao, L., Li, J., Pu, R., Shi, X., Wang, L., Liu, R., Xu, H., Tong, C., Zhou, Z., 2019. Landscape grain effect in Yancheng coastal wetland and its response to landscape changes. Int. J. Environ. Res. Public. Health 16, 2225. https://doi.org/10.3390/ijerph16122225.

Toosi, N.B., Soffianian, A.R., Fakheran, S., Waser, L.T., 2022. Mapping disturbance in mangrove ecosystems: Incorporating landscape metrics and PCA-based spatial analysis. Ecol. Indic. 136, 108718 https://doi.org/10.1016/j.ecolind.2022.108718.

Topaloğlu, R.H., Aksu, G.A., Ghale, Y.A.G., Sertel, E., 2021. High-resolution land use and land cover change analysis using GEOBIA and landscape metrics: A case of Istanbul. Turkey. Geocarto Int. 1–27 https://doi.org/10.1080/10106049.2021.2012273.

Ul Din, S., Mak, H.W.L., 2021. Retrieval of Land-Use/Land Cover Change (LUCC) Maps and Urban Expansion Dynamics of Hyderabad, Pakistan via Landsat Datasets and Support Vector Machine Framework. Remote Sens. 13, 3337. https://doi.org/10.3390/rs13163337.

Wang, H., Li, C., 2021. Analysis of scale effect and change characteristics of ecological landscape pattern in urban waters. Arabian J. Geosci. 14, 1–8. https://doi.org/10.1007/s12517-021-06831-y.

Wang, J., Li, L., Zhang, T., Chen, L., Wen, M., Liu, W., Hu, S., 2021b. Optimal grain size based landscape pattern analysis for Shanghai using Landsat images from 1998 to 2017. Pol. J. Environ. Stud. 30, 2799–2813. https://doi.org/10.15244/pjoes/129702.

Wang, Z., Liu, Y., Li, Y., Su, Y., 2022. Response of Ecosystem Health to Land Use Changes and Landscape Patterns in the Karst Mountainous Regions of Southwest China. Int. J. Environ. Res. Public. Health 19, 3273. https://doi.org/10.3390/ijerph19063273.

Wang, D., Ma, R., Xue, K., Loiselle, S.A., 2019. The assessment of Landsat-8 OLI atmospheric correction algorithms for inland waters. Remote Sens. 11, 169. https://doi.org/10.3390/rs11020169.

Wang, X., Meng, Q., Zhang, L., Hu, D., 2021c. Evaluation of urban green space in terms of thermal environmental benefits using geographical detector analysis. Int. J. Appl. Earth Obs. Geoinf. 105, 102610 https://doi.org/10.1016/j.jag.2021.102610.

Wang, G., Mu, B., Song, P., Jin, M., He, R., Tian, G., 2018. Scale effects on land use patterns in Luohe City based on an unmanned aerial vehicle survey. Acta Ecol. Sin. 38, 5158–5169. https://doi.org/10.5846/stxb201705190927.

Wang, C., Wu, D., Shen, Z., Peng, M., Ou, X., 2021a. How do physical and social factors affect urban landscape patterns in intermountain basins in Southwest China? Landsc. Ecol. 36, 1893–1911. https://doi.org/10.1007/s10980-020-01182-7.

Wu, J., 2021. Landscape sustainability science (II): core questions and key approaches. Landsc. Ecol. 36, 2453–2485. https://doi.org/10.1007/s10980-021-01245-3.

Wu, Q., Guo, F., Li, H., Kang, J., 2017. Measuring landscape pattern in three dimensional space. Landsc. Urban Plann. 167, 49–59. https://doi.org/10.1016/j.landurbplan.2017.05.022.

Xiao, B., Bai, X., Zhao, C., Tan, Q., Li, Y., Luo, G., Wu, L., Chen, F., Li, C., Ran, C., 2023. Responses of carbon and water use efficiencies to climate and land use changes in China's karst areas. J. Hydrol. 617, 128968 https://doi.org/10.1016/j.jhydrol.2022.128968.

Xu, Z., Hu, Y., Liu, Y., Yan, Y., 2012. A review on the accuracy analysis of spatial scaling data. Prog. Geogr. 31, 1574-1582. 10.11820/dlkxjz.2012.12.002.

Xu, C., Pribadi, D.O., Haase, D., Pauleit, S., 2019. Incorporating spatial autocorrelation and settlement type segregation to improve the performance of an urban growth model. Chin Geogr Sci. 47, 1184–1200. https://doi.org/10.1177/2399808318821947.

Xu, C., Zhao, S., Liu, S., 2020. Spatial scaling of multiple landscape features in the conterminous United States. Landsc. Ecol. 35, 223–247. https://doi.org/10.1007/s10980-019-00937-1.

Yang, T., Wang, X., 2021. Evaluation of the plant landscape suitability in mountain parks based on principal component analysis: A case study of Guiyang City. Agron. J. 113, 760–773. https://doi.org/10.1002/agj2.20463.

Yang, J., Yang, J., Xing, D., Luo, X., Lu, S., Huang, C., Hahs, A.K., 2020. Impacts of the remnant sizes, forest types, and landscape patterns of surrounding areas on woody plant diversity of urban remnant forest patches. Urban Ecosyst. 24, 345–354. https://doi.org/10.1007/s11252-020-01040-z.

Yuan, S., Xia, H., Yang, L., 2021. How changing grain size affects the land surface temperature pattern in rapidly urbanizing area: a case study of the central urban districts of Hangzhou City. China. Environ. Sci. Pollut. Res. 28, 40060–40074. https://doi.org/10.1007/s11356-020-08672-w.

Zhang, S., Bai, X., Zhao, C., Tan, Q., Luo, G., Wang, J., Li, Q., Wu, L., Chen, F., Li, C., 2021. Global CO_2 consumption by silicate rock chemical weathering: its past and future. Earth's. Future 9. https://doi.org/10.1029/2020EF001938.

Zhang, S., Bai, X., Zhao, C., Tan, Q., Luo, G., Cao, Y., Deng, Y., Li, Q., Li, C., Wu, L., 2022. Limitations of soil moisture and formation rate on vegetation growth in karst areas. Sci. Total Environ. 810, 151209 https://doi.org/10.1016/j.scitotenv.2021.151209.

Zhang, Q., Chen, C., Wang, J., Yang, D., Zhang, Y., Wang, Z., Gao, M., 2020. The spatial granularity effect, changing landscape patterns, and suitable landscape metrics in the Three Gorges Reservoir Area, 1995–2015. Ecol. Indic. 114, 106259 https://doi.org/10.1016/j.ecolind.2020.106259.

Zheng, Y., Long, H., Chen, K., 2022. Spatio-temporal patterns and driving mechanism of farmland fragmentation in the Huang-Huai-Hai Plain. J. Geog. Sci. 32, 1020–1038. https://doi.org/10.1007/s11442-022-1983-8.

Zhou, X., Hu, C., Wang, Z., 2022. Ecological Response of Urban Forest Carbon Density to Site Conditions: A Case Study of a Typical Karst Mountainous Regions in Southwest China. Forests 13, 1484. https://doi.org/10.3390/f13091484.